ELSEVIER

Ceramics International 28 (2002) 283–292

CERAMICS INTERNATIONAL

www.elsevier.com/locate/ceramint

Densification behaviour, microstructure development and dielectric properties of pure $BaTiO_3$ prepared by thermal decomposition of (Ba,Ti)-citrate polyester resins

Pedro Duran*, Dionisio Gutierrez, Jesus Tartaj, Carlos Moure

Instituto de Cerámica y Vidrio, CSIC, Electroceramics Department, 28500 Arganda del Rey, Madrid, Spain

Received 25 June 2001; received in revised form 5 August 2001; accepted 17 September 2001

Abstract

The thermal decomposition of (Ba,Ti)-citrate polyester resin method was used to prepare high purity $BaTiO_3$ powders. After milling, the green compacts' uniformity was studied using both the SEM observations on surfaces of the fractured green compacts, and the pore size distribution results obtained by using Hg-porosimmetry. The densification behaviour was found to be closely related to the pore distribution in the powder compacts and, thus, the different maxima in the pore size distribution were assumed to be connected to the maxima in the densification rate. The sintering behaviour of $BaTiO_3$ compacts was evaluated using both non-isothermal and isothermal experiments. Microstructural development during sintering at different heating rates was in accordance with the nonuniformity of the green compacts microstructure. Thus, denser areas could favour the development of twinned grains and the discontinuous grain growth process in the $BaTiO_3$ ceramics. Dielectric constants below the Curie temperature were evaluated according to both densification level and grain size. Although a high density, ($\geqslant$99% theoretical) and fine grained, ($\sim$1.01 μm) microstructure of $BaTiO_3$ could be produced by the used method and sintering in air, in which a high dielectric constant, ($\geqslant$5000 at room temperature and 1 kHz) and a dissipation factor as low as 3% was achieved, however, dielectric constant degradation up to about 2500 with increasing grain size, and some fluctuations in the Curie temperature were observed. It was assumed to be a consequence of the inhomogeneous microstructure and the stresses generated through the cubic-tetragonal transition on cooling. © 2002 Published by Elsevier Science Ltd and Techna S.r.l.

Keywords: A. Sintering; B. Microstructure; C. Dielectric properties; D. $BaTiO_3$

1. Introduction

Owing to its high dielectric constant at room temperature, ($\geqslant$1500), stoichiometric high purity submicronised $BaTiO_3$ powders are being widely used for the preparation of dense ferroelectric and piezoelectric bodies, as well as for thin films electronic component materials. From the discovery by Knepkamp and Heywang [1] that the relative permittivity of $BaTiO_3$ ceramics can be increased to about 3500 if the grain size is controlled at $\sim$1 μm, then a fine grained structure is desirable to enhance the dielectric performances. Therefore, the availability of $BaTiO_3$ powders with homogeneous and smaller particle size, ($\leqslant$0.1 μm) is a key factor. Although the preparation of stoichiometric $BaTiO_3$ powders from the thermal decomposition of oxalates, carbonates and citrates has been extensively studied, [2–10], several problems remain, even today, to be solved. The advantages, at least in the case of the oxalates and citrates, is the formation of a complex compound between Ba and Ti with a 1:1 atomic ratio in which the cations are mixed at atomic level and may, with much shorter diffusion paths, convert to $BaTiO_3$ with a particle size in the nanoscale range, ($\leqslant$100 nm) and a cubic structure [3,11–15].

However, many problems may be encountered in processing high-purity stoichiometric and nanocrystalline $BaTiO_3$ powders. For example, the use of small particles, due to the tendency to form agglomerates, can lead to green microstructures with defects that cannot be eliminated during sintering. Therefore, the state of agglomeration, compaction and, even the pore morphology of powders play a crucial role during processing [16,17]. Thus, the agglomeration problems should be minimised in order to better know the powder behaviour during compaction. Although many efforts have been made

* Corresponding author. Tel.: +34-91-8711800; fax: +34-91-8700550.

E-mail address: pduran@icv.csic.es (P. Duran).

0272-8842/02/$22.00
PII: S0272-8842(01)00092-X

leading to enhance green microstructures using different techniques [18–20], there still remain difficulties in trying to clearly understand the sintering behaviour of green compacts made with agglomerated powders [21–23]. To overcome most of the above mentioned problems it would be desirable to have powders with reversible agglomeration–deagglomeration characteristics, i.e. soft agglomerates allowing to better adjust packing and sintering behaviour [24–26].

The present study is undertaken to investigate the powder characteristics, pore size distribution in the green compacts, their effects on the constant rate heating (CRH) sintering behaviour, microstructural evolution during densification and dielectric properties of barium titanate powders obtained by a slightly modified Pechini method [27].

2. Experimental procedure

The $BaTiO_3$ powders with a stoichiometry Ba/Ti = 1, were prepared by a slightly modified Pechini method and the details of the powder synthesis procedure was given elsewhere [15]. The powders were isopressed at 200 MPa without binders, being the green density of the pressed samples 2.95, i.e. about the 49% of the theoretical density, (6.02 g cm^{-3}). Sintering was performed under various conditions of constant rate heating, from 2 to 15 °C/min, in the range of temperature from 25 to 1400 °C. All the sintering conditions experiments were carried out in static air in a differential dilatometer. The apparent density of the sintered samples was measured by the Archimedes method of immersion in water.

The microstructure of the as sintered samples was examined on the polished and thermally etched surfaces by using a scanning electron microscope (SEM). The grain sizes were determined by the line-intercept method [28] and the reported average grain size of a sintered sample corresponds to the main diagonal values of, at least, 300 individual grains.

The dielectric properties were measured at 1 KHz with a LCR meter, (HP 4291 A) at the temperature range from 25 to 200 °C. On both sides of polished samples silver paste was applied and cured at 200 °C. Sample dimensions were determined for dielectric constant calculations. The electrical measurements were carried out during the cooling cycle from 200 to 25 °C, with a cooling rate of 0.5 °C/min.

3. Experimental results

3.1. Powder characterisation and compaction

Fig. 1 shows the morphology of the $BaTiO_3$ powders after calcining at 750 °C for 2 h. Agglomerates, both soft and hard, in the range of 0.5–2 μm in size, dominate the calcined powders, although the discrete particles were in the nanoscale range (⩽100 nm) in all cases. In fact, the specific surface area of the $BaTiO_3$ powders, as determined by single-point BET was about 33 m^2 g^{-1} and the calculated equivalent particle size from the expression $D = 6/\rho S$, (where D is the average diameter of spherical particles, S the surface area of the calcined powder and ρ the theoretical density of $BaTiO_3$), was about 30 nm.

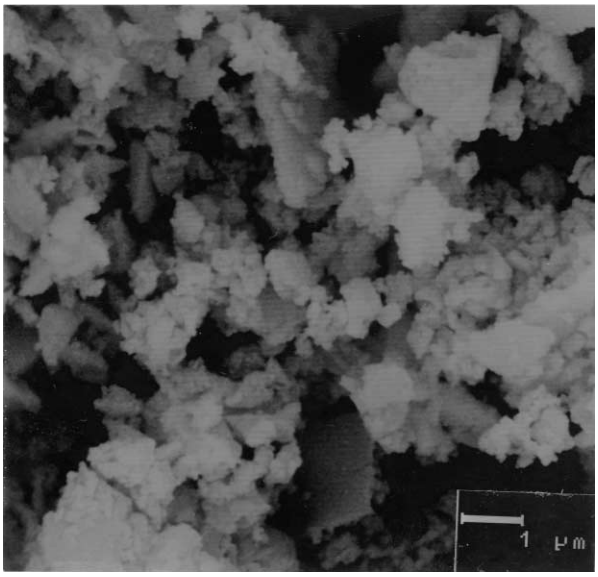

Fig. 1. SEM micrographs of the $BaTiO_3$ nanosized powder calcined at 750 °C.

After compaction the pore size distribution of the powder compacts showed, as it can be seen in the Fig. 2, mainly a bimodal distribution. Such two pore

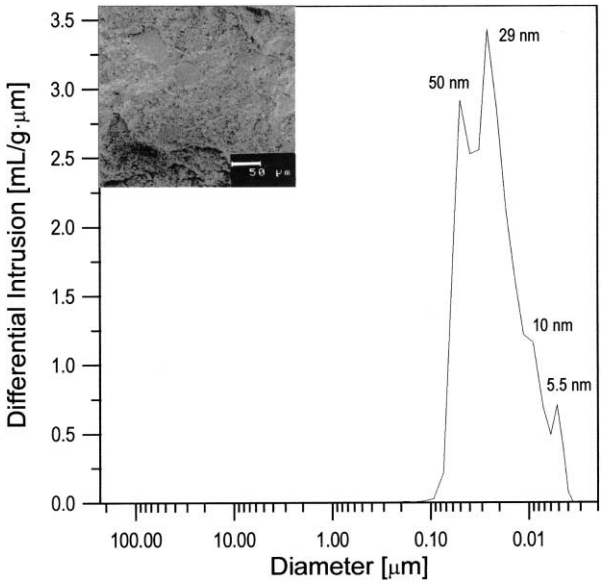

Fig. 2. Pore-size distribution and microstructure for the $BaTiO_3$ green compacts.

size distribution was centred at about 29 and 50 nm, respectively. It indicates that some hard agglomerates have not broken during pressing, leading to the formation of large voids which will be difficult to be eliminated on sintering. It must be noted that in the region of the smaller pores two peaks centred at about 5.5 and 10 nm respectively, were also present. The smaller pores can be attributed to the intraagglomerate porosity. Therefore, it can be said that the major part of porosity can be considered to be present as an interagglomerate or interparticle porosity.

3.2. CRH densification behaviour

Linear shrinkage and differential linear shrinkage curves during CRH, (5 °C/min) sintering are shown in the Fig. 3. The onset of densification was above 850 °C and four sintering stages can be observed at about 880, 940, 1205 and 1220 °C, respectively. Each maximum in the shrinkage rate curve seems to correspond to a peak in the pore size distribution one and, assuming a solid state densification mechanism at this temperature interval, each of them correspond to the elimination of the smaller pores with particle rearrangement, at the lower temperature interval (880–940 °C), i.e. at the earlier sintering step and the larger ones at the higher temperature interval (1205–1300 °C), i.e. at the intermediate sintering step, respectively. Such densification behaviour is in close agreement with the pore size distribution in the green compacts and, as a result, the end densification was displaced to a relatively high temperature, (about 1370 °C). The final density value in the last sintering step approached 99% of the theoretical density. Fig. 4 provides further information on the sintering of these highly reactive $BaTiO_3$ nanosized powders.

Fig. 5 shows the effect of heating rate on the densification behaviour of $BaTiO_3$ compacts. Four relevant

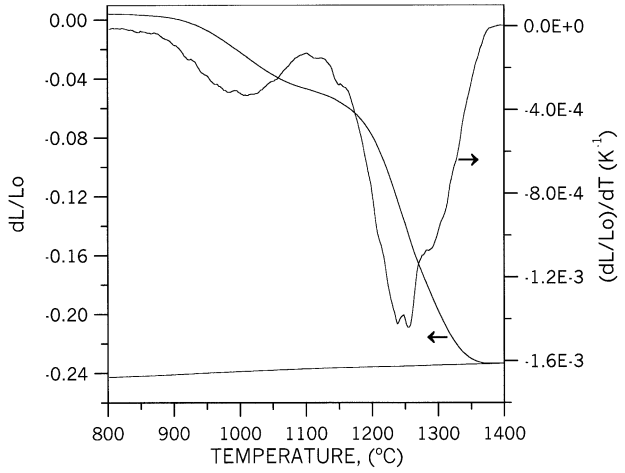

Fig. 3. Densification behaviour under constant-heating-rate (5 °C/min) for pure $BaTiO_3$ green compacts.

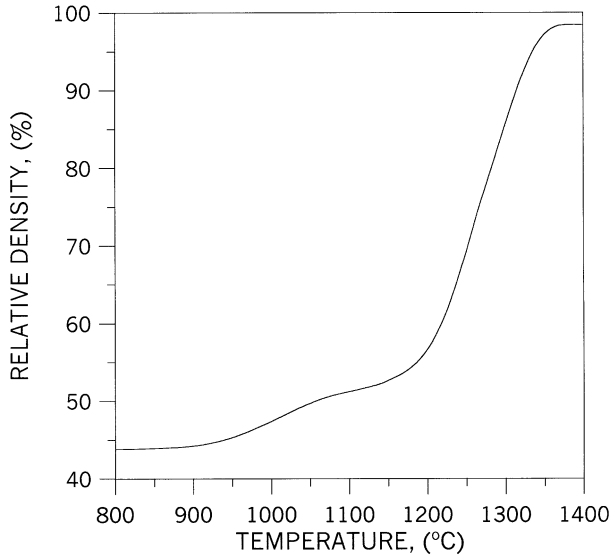

Fig. 4. Sintering curve for nanosized $BaTiO_3$ powder. The constant heating rate was 5 °C/min.

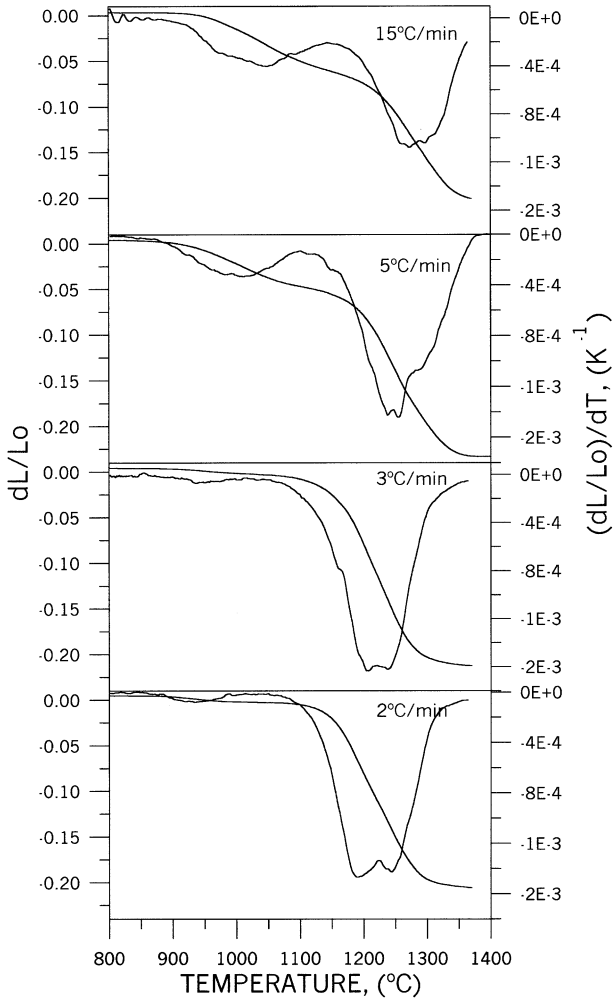

Fig. 5. Sintering curves for the nanosized $BaTiO_3$ powders at different constant heating rate.

features can be observed: (i) the densification is initiated at approximately the same temperature, independent of the heating rate, (ii) the total shrinkage was lower for the higher heating rate, (iii) the shrinkage rate maxima were displaced towards higher temperatures as the heating rate was raised, and (iv) the final density increased with the heating rate up to a value of 5.95 g cm^{-3}, (about 99% theoretical value) for a heating rate of 5 °C/min, and then goes down to 5.85 g cm^{-3} (about 97% theoretical density) when the heating rate was raised up to 15 °C/min.

The densification behaviour of $BaTiO_3$ compacts was further studied under isothermal conditions at 1260 °C, i.e. below the eutectic melt temperature of the $BaTiO_3$–TiO_2 system [29], which is located at about 1312, and 1370 °C, i.e. above the eutectic melt, for sintering times from 0.5 to 10 h. Fig. 6 shows plots of relative density vs sintering time at 1260 and 1370 °C for different heating rate regimes. In the solid state densification region, the densification rate is higher for the samples sintered at the higher heating rate, but a lower density after 1h was attained, (94 against 97%). Above that sintering time a maximal density of 98% after 5 h was achieved, and a slight desintering, (97.5%), was observed after 10 h for the lower heating rate. When the heating rate is raised up to 15 °C/min, the maximal density (94.5%) was attained after 1 h followed by a strong decrease in density after 2 h. The final density decreased up to 92% after 10 h.

In the liquid phase sintering region a maximal density of 97% was attained at 1370 °C without holding time, and such a densification level was maintained after 1 h. For longer sintering times a strong desintering took place and the density decreased up to 94% after 10 h.

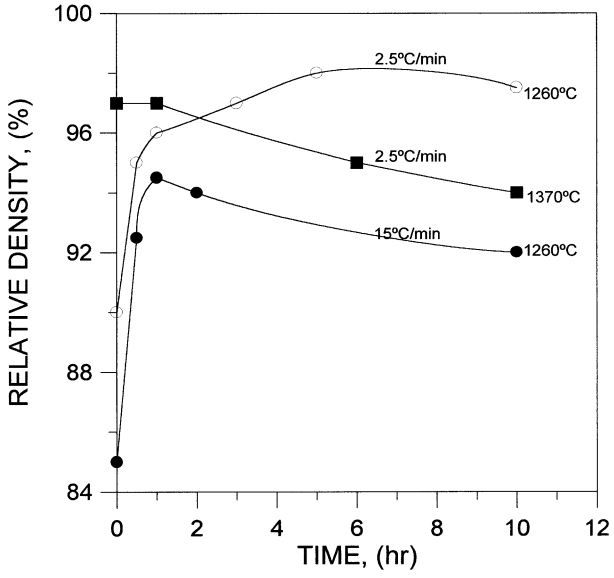

Fig. 6. Density versus time for the nanocrystalline $BaTiO_3$ powder isothermally treated at 1260 and 1370 °C.

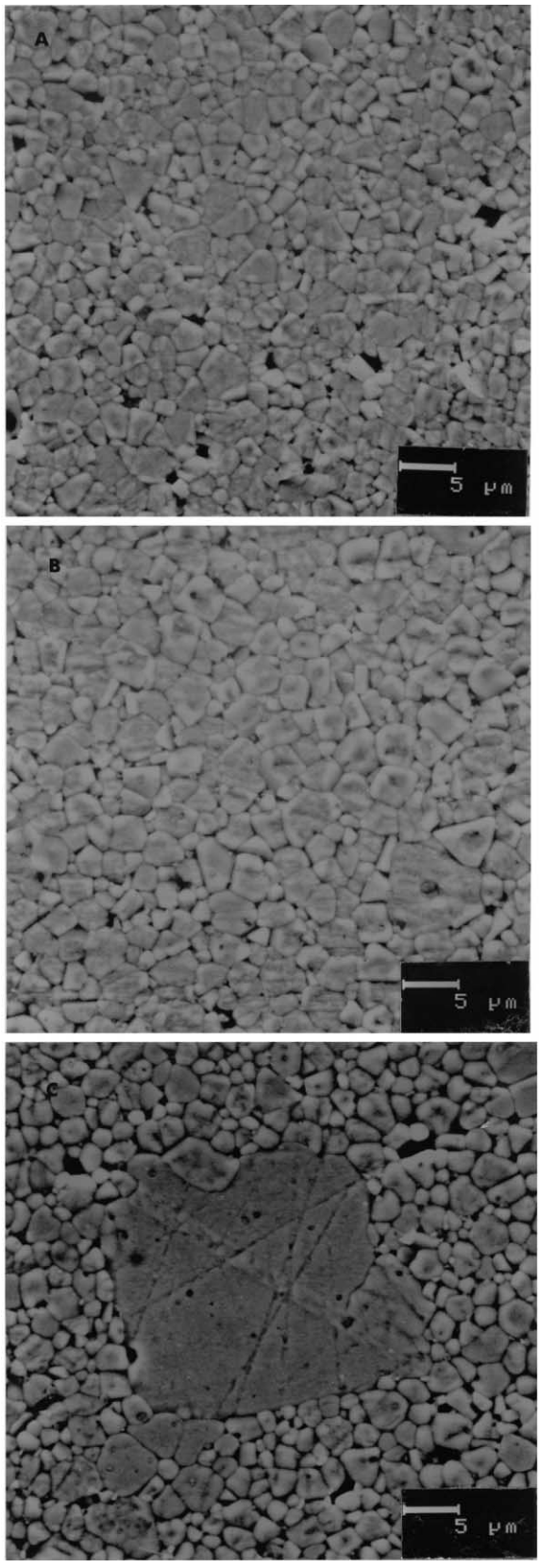

Fig. 7. SEM micrographs of nanosized $BaTiO_3$ powders isothermally sintered at 1260 °C and a heating rate of 2.5 °C/min: (A) $D=96\%$ theoretical; (B) $D=97\%$, and (C) $D=98\%$, showing discontinuous grain growth.

3.3. Microstructural development during sintering

Although several factors can influence on the microstructural features to be developed during sintering, we will take into account the temperature and the sintering time as the main factors controlling the microstructure in those samples sintered above and below the eutectic temperature of the $BaTiO_3$–TiO_2 system. Fig. 7 shows the microstructure of samples sintered at 1260 °C for 1–5 h at a heating rate of 2.5 °C/min. As can be seen, the grain size hardly increases with the sintering time up to 3 h and an abnormal grain growth took place for a sintering time of 5 h. The average grain size was measured to be between 2 and 3 μm in the fine grained ceramic matrix. The anomalous grain size was well above 10 μm. Fig. 8 shows the microstructure of the samples sintered at the same temperature but at a heating rate of 15 °C/min, for 0.5–2 h. The developed microstructure was of polygonized grains with a grain size slightly smaller than those samples sintered at a heating rate of 2.5 °C/min. The only distinguishable fact was the absence of abnormal grain growth at these last sintering conditions. Fig. 9 shows the microstructure of samples sintered above the eutectic temperature of the $BaTiO_3$–TiO_2 system. A common fact, independent of the heating rate, was present in all the samples sintered above 1312 °C, and this is that of a microstructure of abnormally growing grains embedded in a fine grained matrix. Fig. 9(A) is representative of such developed microstructure, in which the grain size of the abnormal grains was four or five times greater than those of the ceramic matrix grains. The final grain size in the ceramic matrix was in all cases about 2.5 μm, as is shown in Fig. 9(B)–(D). A characteristic feature of the samples sintered at a heating rate of 15 °C/min, as shown in the Fig. 9(E) was the presence of a swelling phenomenon as a consequence of gas entrapment. Fig. 9(F) shows a typical grain surface habit plane in the fine-grained matrix. As can be observed, traces of a twin lamella were present in some grains with a thickness of about 0.2 μm.

3.4. Dielectric properties

Table 1 shows the temperature dependence of the permittivity for the $BaTiO_3$ ceramics sintered at different sintering conditions. As can be seen, the grain size has a strong effect on both the Curie temperature and the permittivity but all sets show a maximum at the transition temperature of about 120 ± 2 °C. Although the evolution is in close agreement with other reports in which such a temperature dependence was only attributed to a microstructural factor, i.e. the grain size [30,31] but our results show evidence for a correlation between the crystal structure of the $BaTiO_3$ ceramics and the dielectric properties, without underestimating the influence of the grain size. As is shown, the permittivity increases

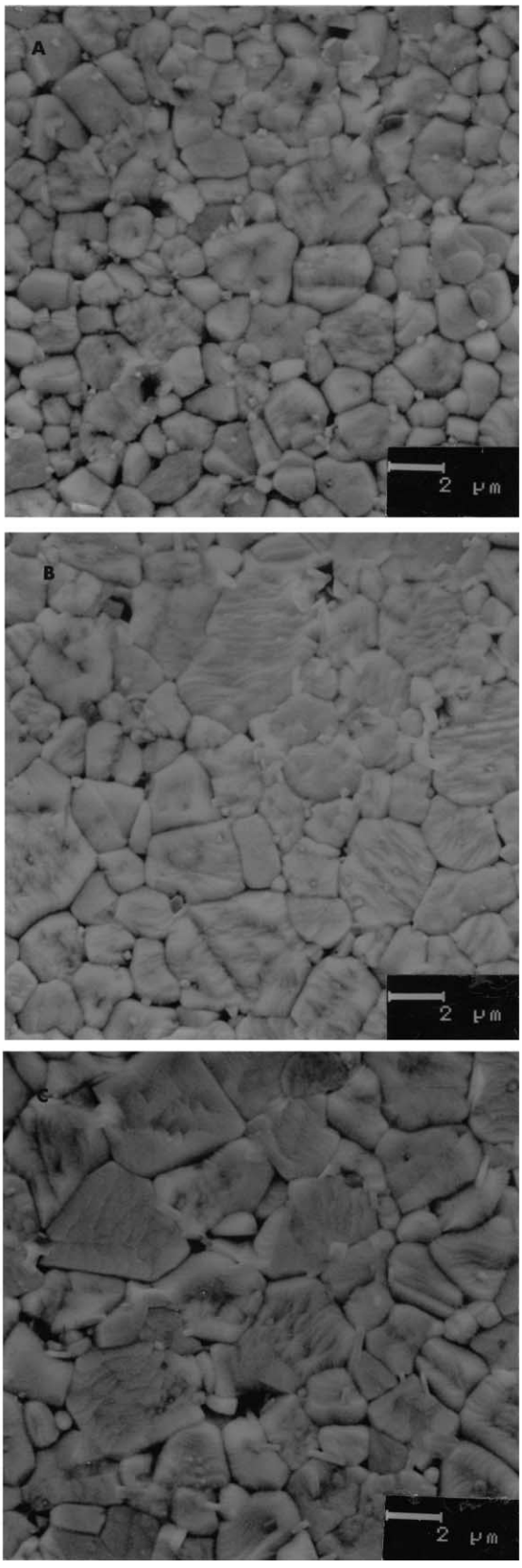

Fig. 8. SEM micrographs of nanosized $BaTiO_3$ powders isothermally sintered at 1260 °C and a heating rate of 15 °C/min: (A) $D = 92.5\%$ theoretical; (B) $D = 94.5\%$, and (C) $D = 94\%$, showing no discontinuous grain growth.

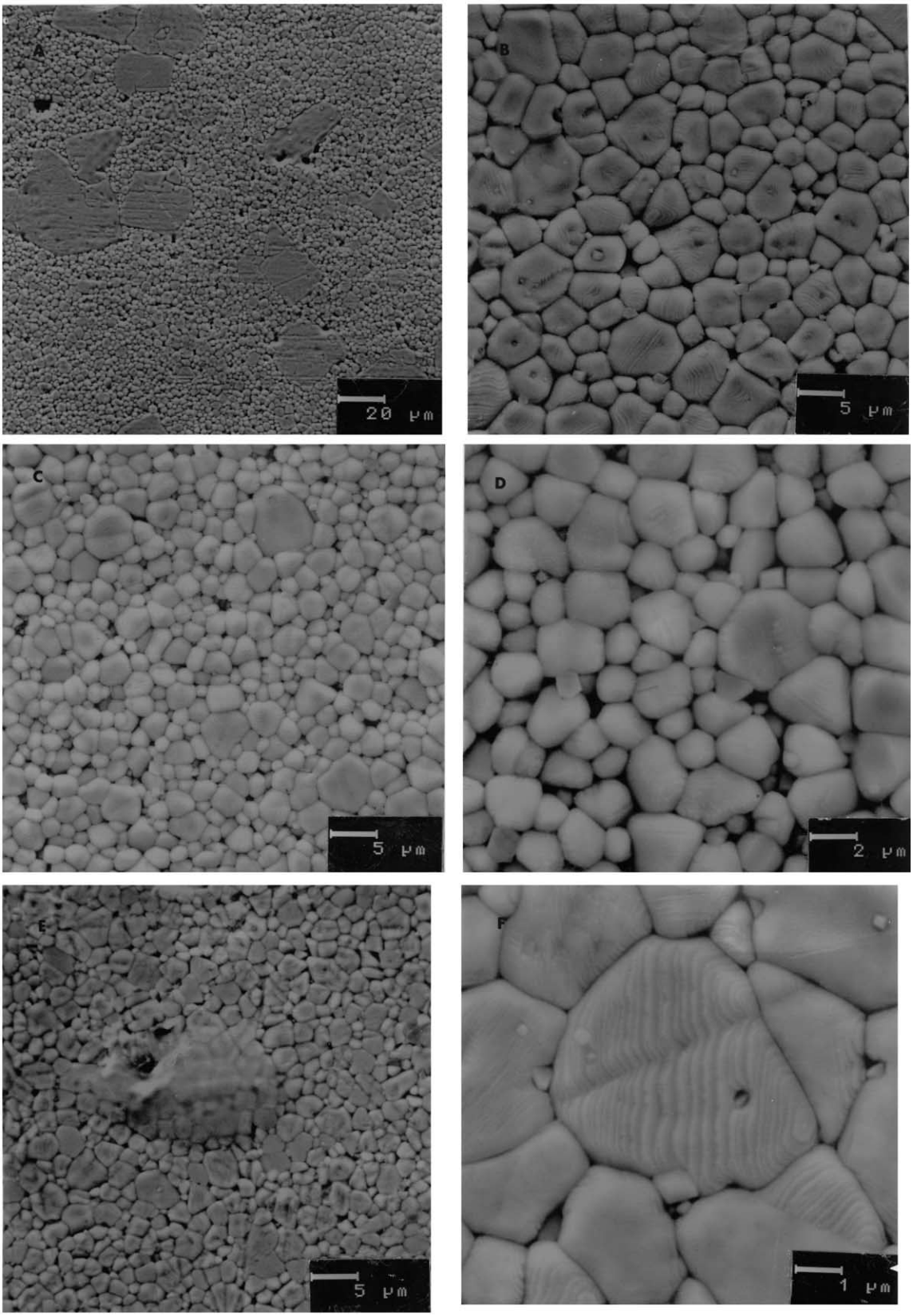

Fig. 9. SEM micrographs of nanosized $BaTiO_3$ powders sintered at 1370 °C without holding, (A) showing a general aspect of the microstructure; (B), (*C*), and (*D*) show the ceramic matrix microstructure of samples sintered at a heating rate of 2, 5 and 15 °C/min, respectively, showing several twin lamella and twined grains; (E) shows the swelling phenomenon observed in samples sintered at 15 °C/min, and (F) sintered sample showing a clear trace of twin lamella.

Table 1
Dielectric properties for $BaTiO_3$ ceramics sintered at different temperatures

Temperature (°C)	Density (%)	Grain size (μm)	Dielectric constant		Curie temperature (°C)
			RT	T_C	
1260–0 h	96	1.01	>5500	10000	120
1285–2 h	99	2	2200	9500	110
1285–10 h	98	3.2	2340	10000	112
1370–0 h*	97	1.9	3650	12800	110
1370–0 h#	97.5	1.8	≈5000	15800	112

* Heating rate, 2 °C/min.
# Heating rate, 3 °C/min.

with the grain size decreasing and a maximal permittivity was attained when the grain size reached ~1 μm and the abnormal grain growth was restricted. The higher permittivity value at room temperature and 1 kHz (⩾ 5000) was achieved for a sintering temperature of 1260 °C, and the grain size in such a sample, as shown in the Fig. 10, was about 1.01 μm. The dissipation factor was, in all cases, slightly less than 3%, which is similar to those reported in other papers [32,33].

4. Discussion

The above obtained results on a $BaTiO_3$ powder produced by a slightly modified Pechini method indicated that such a powder was strongly agglomerated which, after compaction the relatively high strength of some agglomerates led to green compacts with a bimodal pore size distribution, see Fig. 2. As a consequence of the resistance of hard agglomerates to be broken during pressing, this heterogeneous green microstructure gave rise to the formation of two distinct areas, one more dense than the other. Thus, with the mentioned two pore size distribution in which the peaks corresponding to the larger pore sizes are considered to be generated by large interagglomerate pores, we can suggest that the presence of different kinds of agglomerates in the $BaTiO_3$ powders gives rise to a broader inhomogeneous pore size distribution.

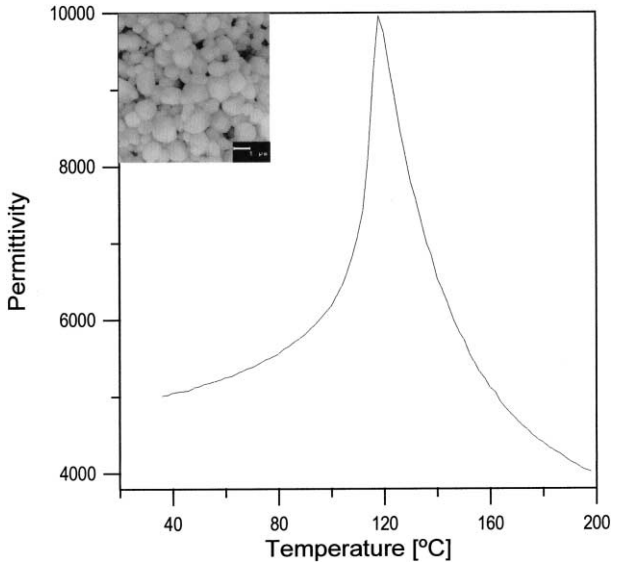

Fig. 10. Temperature dependence of the dielectric constant of nanosized $BaTiO_3$ sample sintered at 1260 °C with the highest room temperature value (⩾5000), and the best grain size (1.01 μm).

From Figs. 3 and 4 it seems clear that a good correlation exists between the pore size distribution and the densification behaviour of the $BaTiO_3$ green compacts. The smaller pores are eliminated at the lower temperatures but their volume is not sufficiently high as to provoke a strong shrinkage of the green compacts. In fact, the elimination of the smaller pores, or intraagglomerate porosity, from the beginning of the earlier sintering steps, at about 960–980 °C, does not produce a shrinkage higher than about 5%. The larger pores, or interagglomerate porosity, need higher temperatures to be eliminated [34]. Thus, a rapid shrinkage takes place above 1100 °C for the different heating rates with a small grain growth, indicating that the main densification of the samples took place in the intermediate stage of sintering, see Fig. 3. It is interesting to point out that at the lower heating rate (2.5 °C/min), a discontinuous grain growth was observed when the sintering time was larger than 5 h and the density was about 97% theoretical. On the contrary, for the higher heating rate (15 °C/min), no abnormal grain growth was observed within the sintering time interval here studied, although the sintering density was not higher than 94% theoretical, see Fig. 6. These results indicate some correlation between sintering density and abnormal grain growth [35,36]. Hsieh and Fang [37], found that abnormal grain growth was only present for sintering density >99% theoretical. However, if most of the porosity is eliminated, as is the present case, the anomalous grain growth can take place beyond a critical value of the density, thus supporting the Coble and Gupta suggestions [35,36]. This is thought to occur in the samples sintered in the solid-state at a heating rate of 15 °C/min (see Fig. 6), in which the sintering density was about 94% theoretical. Based on the present results we estimate that for a density level

higher than 96% theoretical, the anomalous grain growth takes place when the samples are sintered in the solid-state region, i.e. below the eutectic temperature of the TiO_2–$BaTiO_3$ system, for a relatively short time (≈2 h). This statement is contradictory to that of Schmelz and Meyer [38], who postulated an anomalous grain growth by solid-state mechanism attributed to the formation of twinned crystals in a dense matrix as a necessary requirement, but our results are in close agreement with those of Hsieh and Fang [37], obtained on agglomerated samples previously calcined at 1300 °C. Xue and Brook [39] attributed a short-term increase in densification to an abnormal grain growth process, interpreting that such a densification rate enhancement cannot be related to the presence of a liquid phase, but rather to a favourable influence of abnormally increased grain size on the thermodynamic driving force for densification. It must be noted that their results were also obtained on $BaTiO_3$ samples sintered at 1290 °C, which is below the eutectic temperature of the $BaTiO_3$–TiO_2 system. At this point it must be indicated that no twinned grains were observed in our samples with a sintering density lower than 96% theoretical and a grain size smaller than 2 μm. Then it should be assumed that if to initiate the anomalous grain growth process a twinning phenomenon is required, then a critical grain size for the formation of twins detectable on the grain surfaces has to exist above which the abnormal grain growth process is triggered. Schmelz and Meyer [38] considered that density of the samples was not a factor to take into account for the abnormal grain growth process, since this phenomenon was already present in a 65% dense sample. However, in some cases, in spite of the presence of a twinning phenomenon, not all the twinned grains grew further, i.e. only a few grains are able to continue growing. Therefore, it should be assumed that not only a critical grain size for the development of anomalous grains would be necessary but a minimal densification level would also trigger the anomalous grain growth process. Hsieh and Fang [37] denied the necessary presence of a twinning phenomenon for the development of the anomalous grain growth process. At any case, it is clear that normal grain growth in undoped $BaTiO_3$ ceramics sintered in the solid-state region is quite slow within a density range (see Fig. 9).

Sintering above the eutectic point at 1312 °C, in the hypothesis of the existence of excess TiO_2 in the sintered samples, our results have shown that, independent of the heating rate and sintering time, an abnormal grain growth process takes place in all cases [see Fig. 9(A)], showing the abnormally growing grains. In some cases, a single-twin located nearly at the middle of each grain can be seen. The exaggerated grain growth of $BaTiO_3$ when the samples are sintered in the liquid phase region could be explained by an Ostwald ripening process if all the $BaTiO_3$ grains are wetted by a liquid phase thin film, i.e. if the volume of the formed liquid phase is sufficiently high. In the present case, in which the stoichiometric deviation was, if any, very small, the amount of the formed liquid phase was so small that the abnormal grain growth process would be rather favoured by the initial number of nuclei (twinned grains) in the sample. The presence of twinned grains heterogeneously distributed in our $BaTiO_3$ sintered samples supported the above contention which, on the other hand, is in close agreement with previous suggestions [38,39]. Furthermore, it must be mentioned that the formation of abnormally growing grains does not enhance the densification at least in the final sintering stage which is contrary to that postulated by Xue and Brook [39]. Our results showed evidence, as shown in the Fig. 9E, that a certain bloating phenomenon was present in the samples sintered at the higher heating rate in the liquid phase region, giving rise to grain growth and pore coalescence, and, as consequence, to a decreasing in the density [40]. A heterogeneous phase equilibria with evolution of entrapped gas could be the cause for such a dedensification process [41].

From the above results and comparing them with the well known role of (111) twins in abnormal grain growth for $BaTiO_3$ ceramics containing an excess of TiO_2 [42,43], it can be concluded that both the experimental conditions for (111) twin formation and the formation mechanism are not still unambiguously explained. For nanosized powders, as is the present case, (crystallite size ≈ 30 nm), it was pointed out that although the bulk structure of $BaTiO_3$ powder appeared cubic, but the Raman characterisation showed the presence of a tetragonal structure for such a small particle size [15]. This being so, the appearance of a twinning phenomenon already in the calcined powders could be reasonably assumed [42]. The measure in which the twinned grains are favourably rotated during the particle rearrangement in the initial sintering stages, leading to the formation of a twin lamella as a nucleus for the discontinuous grain growth would trigger such a process. However, for nanosized powders the diffusion paths are much shorter, and the normal grain growth by grain boundary diffusion can be favoured between the smaller particles. If these small particles are not uniform in size, then the larger particles can grow in an anisotropic manner at the expenses of the smaller ones up to a critical grain size above which a twinning phenomenon can also be present. In those initially twinned grains, the formation of a twin lamella, acting as a nucleus, would favour the anomalous grain growth process according to the sintering schedule and other experimental conditions. In summarising, we suggest that in undoped-$BaTiO_3$ nanosized powders with no excess of TiO_2, the global grain growth process could take place in two different ways, (i) the grains with an initial averaged pseudocubic structure can normally grow by a grain boundary

diffusion, and (ii) in the grains having already in the calcined powders a twinned tetragonal structure met all the favourable conditions for an anomalous grain growth process during sintering, as postulated by Kastner et al. [44]. This suggestion is in agreement with the microstructure shown in the Fig. 9(D), in which two kinds of grains, (twinned and untwinned) are present. Therefore, the necessary conditions for the formation of (111) twins in $BaTiO_3$ ceramics claimed by Lee et al. [45] could not be recognised as the only cause.

As shown in Table 1, the grain size influences the dielectric constant of the $BaTiO_3$ ceramics in such a way that it is strongly degraded when the grain size increases above 1 μm. Some small fluctuations were also observed in the Curie transition temperature, (T_c). These features are in close agreement with the suggestions of Arlt et al. [30] and Takeuchi et al. [46], which emphasised the decreasing of the dielectric constant below and above a critical grain size, ($\sim$0.8 μm). Such behaviour was attributed to domain size effects and/or to a ferroelectric structure change. In our case, in which a relatively wide grain size range was a current characteristic of the $BaTiO_3$ sintered samples, it is believed that although the bulk structure can be considered as a tetragonal one, but the presence in the final microstructure of many small grains ($\leqslant$0.5 μm) with a probable cubic structure, could give rise to a lower dielectric constant and a distribution of transition temperatures. As a consequence, the internal stresses heterogeneously distributed in the system can explain the small changes of the Curie temperature in the $BaTiO_3$ sintered samples [47]. Some broadening of the dielectric constant peak supported the above statement. In such finer grains the absence of twins can strongly affect the internal stresses of the system and, therefore, the dielectric properties of the $BaTiO_3$ ceramics [48].

5. Conclusions

It has been established that the high purity $BaTiO_3$ nanosized powders prepared by thermal decomposition of (Ba,Ti)-citrate polyester resins are highly agglomerated. After milling, the agglomerates strongly determined the compaction behaviour and, depending on the agglomerates strength, some of them survived after compaction leading to heterogeneous pore size distribution in the green compacts.

On non-isothermal sintering in air (at a heating rate of 5 °C/min) the smaller pores are eliminated at the lower temperatures, i.e. in the earlier sintering stages up to 1100 °C, with a rearrangement particle process. Such a process led to a new pore size configuration which favoured the larger pores elimination and rapid densification during the intermediate sintering stage, i.e. up to about 1300 °C, with a slow grain growth. Above 1300 °C, the final sintering stage, dense $BaTiO_3$ ceramic bodies, ($\geqslant$99% theoretical density) were obtained and an abnormal grain growth process took place.

From the isothermal sintering experiments up to 1260 and 1370 °C at different heating rates (2.5 and 15 °C/min), it can be stated that in the low temperature region treatment the densification rate increased as the heating rate increased and the grain growth decreased, but the final density was lower. No abnormal grain growth at the higher heating rate was observed. In the high temperature treatment the final density increased with decreasing heating rate and an abnormal grain growth process was always present, independently of the heating rate.

According to the microstructural development during sintering it can also be stated that a minimal densification level, ($\sim$96% theoretical), and a critical grain size, ($\leqslant$1 μm) are necessary for the development of twinned and discontinuous grain growth in pure $BaTiO_3$ ceramics.

Although the best dielectric constant, ($\geqslant$5000) was found for $BaTiO_3$ ceramics with a grain size of about 1 μm, both the dielectric constant and the Curie temperature degraded and lowered, respectively, as consequence of a higher grain size, heterogeneities in the microstructure, and the stresses generated during the cubic-tetragonal transition on cooling.

Acknowledgements

This work was supported by the Spanish CICYT-MAT-97-0679-C02-01.

References

[1] H. Kniepkamp, W. Heywang, Depolarisation effects in polycrystalline $BaTiO_3$, Z. Angew. Phys. 6 (9) (1954) 385–390.
[2] L.K. Templeton, J.A. Pask, Formation of $BaTiO_3$ from $BaCO_3$ and TiO_2 in air and in CO_2, J. Am. Ceram. Soc. 42 (5) (1959) 212–216.
[3] W.S. Clabaugh, E.M. Swiggerd, R. Gilchrist, Preparation of titanyl oxalate tetrahydrate for conversion to barium titanate of high purity, J. Res. Nat. Bur. Stand. 56 (5) (1956) 289–291.
[4] H. Yamamura, A. Watanabe, S. Shirasaki, Y. Moriyoshi, A. Tanada, Preparation of barium titanyl oxalate method in ethanol solution, Ceram. Int. 11 (1) (1985) 17–22.
[5] K. Kiss, J. Magder, M.S. Vukasovic, R.J. Lockhart, Ferroelectricity of ultrafine particle size, J. Am. Ceram. Soc. 49 (6) (1966) 291–295.
[6] M.S. Stokenhuber, H. Mayer, J.A. Lercher, Preparation of barium titanate from oxalates, J. Am. Ceram. Soc. 76 (5) (1993) 1185–1190.
[7] D. Hennings, W. Mayr, Thermal decomposition of (Ba,Ti) citrates into barium titanate, J. Solid. State Chem. 26 (1978) 329–338.
[8] J.P. Coutures, P. Odier, C. Proust, Barium titanate formation organic resins formed with mixed citrates, J. Mater. Sci. 27 (1992) 1849–1856.
[9] S. Kumar, G.L. Messing, W. White, Metal organic resin derived barium titanate: I, formation of barium titanium oxycarbonate intermediate, J. Am. Ceram. Soc. 76 (3) (1993) 617–624.

[10] M. Rajendran, M. Subba Rao, Formation of $BaTiO_3$ from citrate precursors, J. Solid State Chem. 113 (1994) 239–247.
[11] K.S. Mazdiyasni, R.T. Dolloff, J.S. Smith, Preparation of high purity submicron barium titanate powders, J. Am. Ceram. Soc. 52 (10) (1994) 523–526.
[12] F.S. Yen, T. Chang, Y.H. Chand, Characterisation of barium titanyl oxalate tetrahydrate, J. Am. Ceram. Soc. 73 (11) (1990) 3222–3227.
[13] G. Busca, V. Buscaglia, M. Leoni, P. Nanni, Solid-state and surface spectroscopic characterisation of $BaTiO_3$ fine powders, Chem. Mater. 6 (1994) 955–961.
[14] I.J. Clark, T. Takeuchi, N. Ohtori, D.C. Sinclair, Hydrothermal synthesis and characterisation of $BaTiO_3$ fine powders: precursor polymorphism and properties, J. Mater. Chem. 9 (1999) 83–91.
[15] P. Duran, F. Capel, J. Tartaj, C. Moure, $BaTiO_3$ formation by thermal decomposition of a (Ba,Ti)-citrate polyester resin in air, J. Mater. Res. 16 (1) (2001) 1–13.
[16] D.E. Niesz, R.B. Bennet, Structure and properties of agglomerates, in: G.Y. Onoda, L.I. Hench (Eds.), Ceramic Processing before Firing, John Wiley, New York, 1978, pp. 61–74.
[17] T.T. Fang, H. Palmour III, Useful extensions of the statistical theory of sintering, Ceram. Int. 15 (1984) 329–335.
[18] E.A. Barringer, H.K. Bowen, Formation, packing and sintering of monodisperse TiO_2 powders, J. Am. Ceram. Soc. 62 (12) (1982) c–119-c-121.
[19] I.A. Askay, Microstructure control through colloidal consolidation, in: J.A. Mangles, G.L. Messing (Eds.), Advances in Ceramics, Vol. 9, Forming in Ceramics, American Ceramic Society Inc, Columbus, OH, 1984, pp. 94–104.
[20] F.F. Lange, K.I. Miller, Pressure filtration: consolidation kinetics and mechanisms, Am. Ceram. Soc. Bull. 66 (10) (1987) 1498–1504.
[21] H.L. Hsieh, T.T. Fang, Effects of powder processing on the green compacts of high purity $BaTiO_3$, J. Am. Ceram. Soc. 72 (1) (1989) 142–145.
[22] G.Y.Jr. Onoda, Green body characteristics and their relationship to finished microstructure, in: R.M. Fulrath, J. Pask (Eds.), Ceramic Microstructures, Westview Press, Boulder, CO, 1976, pp. 163–181.
[23] J.P. Smith, G.L. Messing, Sintering of bimodally distributed alumina powders, J. Am. Ceram. Soc. 67 (4) (1984) 238–242.
[24] T.T. Fang, H. Palmour III, Evolution of powder morphology in the sintering of powder compacts, Ceram. Int. 16 (1990) 1–10.
[25] F. Chaput, J.P. Boilot, A. Beauger, Alcoxide-hydroxide route to synthesise $BaTiO_3$-based powders, J. Am. Ceram. Soc. 73 (4) (1990) 942–948.
[26] P. Duran, M. Villegas, F. Capel, P. Recio, C. Moure, Low-temperature sintering and microstructural development of nanocrystalline Y-TZP powders, J. Eur. Ceram. Soc. 16 (1996) 945–952.
[27] M.P. Pechini, Barium titanium citrate, barium titanate and processes for producing the same. US Patent No. 3 231 328, 25 January 1966.
[28] R.L. Fullman, Measurement of particle size in opaque bodies, J. Metal Trans. AIME 197 (1953) 447–452.
[29] H.M. O'Bryan, J. Thomson, Phase equilibria in the TiO_2-rich region of the BaO-TiO_2 System, J. Am. Ceram. Soc. 57 (12) (1974) 522–526.
[30] G. Arl, D. Hennings, G. De With, Dielectric properties of fine grained barium titanate ceramics, J. Appl. Phys. 58 (4) (1985) 1619–1625.
[31] G. Caboche, J.C. Niepce, Dielectric constant of fine grained $BaTiO_3$, in: K.M. Nair, J.P. Gupta, A. Okamoto (Eds.), Ceramic Transactions, Vol. 32, Dielectric Ceramics: Processing, Properties and Applications, American Ceramic Society Inc, Westerville, OH, 1993, pp. 339–345.
[32] J. Novotny, M. Rekas, Dielectric ceramic materials based on alkaline earth metal titanates, Key Eng. Mater. 66/67 (1996) 45–143.
[33] T. Takeuchi, M. Tabuchi, H. Kageyama, Y. Suyama, Preparation of dense $BaTiO_3$ ceramics with submicrometer grains by spark plasma sintering, J. Am. Ceram. Soc. 82 (4) (1999) 939–943.
[34] A. Roosen, H. Hausner, Sintering kinetics of ZrO_2 powders, in: N. Claussen, M. Rühle, A.H. Heuer (Eds.), Advances in Ceramics, Vol. 12, Science and Technology of Zirconia, II, American Ceramic Society Inc, Columbus, OH, 1984, pp. 714–726.
[35] T.K. Gupta, Possible correlation between density and grain size during the sintering, J. Am. Ceram. Soc. 55 (5) (1972) 276–277.
[36] S.C. Samanta, R.L. Coble, Correlation of grain size and density during intermediate-stage sintering, J. Am. Ceram. Soc. 55 (11) (1972) 583.
[37] H.L. Hsieh, T.T. Fang, Effect of green states on sintering behaviour and microstructural evolution of high-purity barium titanate, J. Am. Ceram. Soc. 73 (6) (1990) 1566–1573.
[38] H. Schmelz, A. Meyer, The evidence for anomalous grain growth below the eutectic temperature in $BaTiO_3$ ceramics, Ber. Deuch. Keram. Gess. 8/9 (1982) 436–440.
[39] L.A. Xue, R.J. Brook, Promotion of densification by grain growth, J. Am. Ceram. Soc. 72 (2) (1989) 341–344.
[40] N. Demartin, C. Herard, C. Carry, J. Lemaitre, Dedensification and anomalous grain growth during sintering of undoped barium titanate, J. Am. Ceram. Soc. 80 (5) (1997) 1079–1084.
[41] A.A. Solomon, F. Hsu, Swelling and gas release in ZnO, J. Am. Ceram. Soc. 63 (7/8) (1980) 467–474.
[42] O. Eibl, P. Pongrazt, P. Salicky, Formation of (111) twins in $BaTiO_3$ ceramics, J. Am. Ceram. Soc. 70 (8) (1987) C–195-C-197.
[43] H. Schmelz, H. Thomann, Twinning in $BaTiO_3$ ceramics, Ceram. Forum Int. 61 (1984) 199–204.
[44] G. Kastner, R. Wagner, V. Hillarius, Nucleation of twins by grain coalescence during sintering of $BaTiO_3$ ceramics, Phil. Mag. A 69 (6) (1993) 1051–1071.
[45] B.K. Lee, S.Y. Chung, S.J.L. Kang, Necessary conditions for the formation of (111) twins in barium titanate, J. Am. Ceram. Soc. 83 (11) (2000) 2858–2860.
[46] T. Takeuchi, M. Tabuchi, K. Ado, K. Homjo, O. Nakamura, Y. Suyama, N. Ohtori, M. Nagasawa, Grain size dependence of dielectric properties of ultrafine $BaTiO_3$ prepared by a sol–gel method, J. Mater. Sci. 32 (1997) 4053–4060.
[47] A.J. Bell, A.J. Moulson, The effect of grain size on the dielectric properties of barium titanate ceramics, Br. Ceram. Proc. 36 (1985) 57–66.
[48] A. Yamaji, Y. Enomoto, K. Kinoshita, T. Murakami, Preparation, characterisation and properties of Dy-doped small-grained $BaTiO_3$ ceramics, J. Am. Ceram. Soc. 60 (3/4) (1977) 97–101.